Effect of Worn Top Compression Ring and Lubricant Degradation Towards Engine In-Cylinder Frictional Losses

Article history
Received
20th January 2025
Received in revised form
5th April 2025
Accepted
18th June 2025
Published
26th June 2025

Nur Aisya Affrina Mohamed Ariffin[a]* Jia Yii Tan[a], Chiew Tin Lee[b], William Woei Fong Chong[a,c]

[a]Faculty of Mechanical Engineering, Universiti Teknologi Malaysia, 81310 UTM Johor Bahru, Johor, Malaysia
[b]Faculty of Engineering, Universiti Malaysia Sarawak (UNIMAS), Kota Samarahan 94300, Sarawak, Malaysia
[c]Automotive Development Centre (ADC), Institute for Sustainable Transport (IST), Universiti Teknologi Malaysia, 81310 UTM Johor Bahru, Malaysia

*Corresponding author
nuraisyaaffrina@gmail.com

Abstract

Friction occurs in the internal combustion engine especially at the interface between piston ring and cylinder liner. This causes an increase in fuel consumption required to overcome these frictional losses. Piston ring-cylinder interface is one of the primary sources. This study is imperative to understand the effects of lubrication degradation and worn top compression ring towards engine frictional losses. A mathematical model with the integration of 1-D Reynold's equation is derived to investigate the lubrication film and pressure generation. This study further incorporates velocity, surface roughness, combustion pressure, lubrication degradation and presence of worn top compression ring to demonstrate the frictional losses. It was found that lubrication degradation significantly affects the lubrication film formation, impacting friction at the piston ring-cylinder liner interface. Increased lubricant viscosity increases viscous friction while reducing boundary friction. Similarly, a worn top compression ring leads to higher viscous friction due to a thicker film and larger load-bearing area, decreasing boundary friction. It is concluded that both lubrication degradation and worn top compression rings have detrimental effects on frictional power losses.

Keywords

Piston ring lubrication, Film thickness, Friction, Power loss.

Introduction

Frictional losses in internal combustion engines (ICEs) are a major contributor to energy inefficiency. Up to 40% of the engine's output is lost to internal friction, and roughly 45% of this occurs within the piston system [1]. Within this system, the interface between the top compression ring and the cylinder liner plays a critical role in maintaining sealing, heat transfer, and controlling oil consumption [2].

During engine operation, the top compression ring undergoes significant mechanical and thermal loading, which leads to wear and changes in the ring profile. These changes alter the pressure distribution and film formation at the interface, contributing to increased friction and reduced efficiency [3][4]. At the same time, engine lubricants degrade under high temperatures and through chemical oxidation, which affects viscosity and film thickness, further disrupting lubrication [5][6].

These combined effects can cause a transition from hydrodynamic to mixed or boundary lubrication regimes, particularly near top dead centre (TDC) and bottom dead centre (BDC), where piston velocity is low and oil entrainment is limited [6]. This makes the ring–liner contact zone especially prone to frictional losses and wear at reversal points.

Numerous studies have examined the effects of ring geometry, surface topography, and lubrication on tribological performance [7][8]. While much attention has been given to ring shape and lubricant characteristics individually [9][10], relatively fewer works have addressed the combined impact of ring wear and lubricant degradation over the full engine cycle [3][4]. A dynamic model is required to accurately capture these transient effects and assess frictional performance under real-world operating conditions [11].

This paper presents a numerical study using a one-dimensional Reynolds equation integrated with a Greenwood–Williamson-based rough surface model to investigate the frictional behaviour of a worn top compression ring under degraded lubricant conditions. The simulation aims to predict variations in pressure, film thickness, and friction force across the engine cycle, offering insights into how surface wear and lubricant ageing impact ring–liner interactions.

METHODOLOGY

1-D Reynolds Equation

A mathematical model based on the Reynolds equation is used to analyse the piston ring and cylinder conjunction. The equation is simplified into a one-dimensional form and further reduced using dimensionless quantities, Equation (1). The model predicts the film thickness, pressure distribution, and friction force considering the piston speed. The governing Reynolds equation is given as:

$$\frac{\partial}{\partial X}\left(H^3\frac{\partial P}{\partial X}\right)=\psi\left\{\frac{\partial}{\partial X}(HU)\right\} \tag{1}$$

where $\psi=\frac{12U_{avg}\eta_0 R_x^2}{P_h b^3}$. The equation consists of a left-hand side representing the Poiseuille pressure-induced term and a right-hand side representing the Couette velocity-induced term. The Couette velocity term is simplified as $u=\frac{(u_A+u_B)}{2}$, where u represents the average velocity between the contacting surfaces. This equation focuses solely on lubrication behavior in the x-direction and disregards variations in the y-direction. Any changes in one term will affect the other term and overall lubrication dynamics.

The current model adopts a one-dimensional, steady-state form of the Reynolds equation to analyse the hydrodynamic behaviour within the piston ring–liner conjunction. This simplification allows analysis of film thickness, pressure distribution, and friction force, particularly in the x-direction.

Method of Solution

The Reynolds equation (2) is numerically solved using the finite difference method and expanded through nodal form, *i*. The central finite difference method is used for the left side of the equation, while the backward finite difference method is used for the right side of the equation. Modified Newton Raphson method and Taylor expansion series method were also being applied.

By assuming the residual term approaches zero, it is rearranged to form Equation (3). The term ΔP_i is used with the relaxation factor Ω to calculate the next iteration pressure according to Equation (4), where n represents the iteration number.

$$\Delta P_i=\frac{-F_i-J_1\Delta P_{i-1}-J_0\Delta P_{i+1}}{J_2} \tag{4}$$

$$P_i{}^n=P_i{}^{n-1}+\Omega\Delta P_i{}^n \tag{5}$$

Jacobian term for hydrodynamic lubrication problem are derived as below:

$$J_0=\bar{J}_{i,i+1}=\frac{dF_i}{dP_{i+1}}=\frac{1}{2\Delta X^2}\left(H_{i+1}^3+H_i^3\right) \tag{6}$$
$$J_1=\bar{J}_{i,i-1}=\frac{dF_i}{dP_{i-1}}=\frac{1}{2\Delta X^2}\left(H_i^3+H_{i-1}^3\right)$$
$$J_2=\bar{J}_{i,i}=\frac{dF_i}{dP_i}=-\frac{1}{2\Delta X^2}\left(H_{i+1}^3+2\left(H_i^3\right)+H_{i-1}^3\right)$$

The load acting on a piston ring-cylinder conjunction is a force exerted on the assembly, typically along the x-axis. Understanding the direction and magnitude of this load is crucial for designing and maintaining the system effectively. It allows engineers to optimize performance, durability, and efficiency. Equation (7) is used to calculate the load exerted by the piston ring in this study.

$$Load=\sum_{i=1}^{M-1}Pdx\,R_w \tag{7}$$

Piston Speed

The piston speed is crucial as it affects the lubricant film thickness and pressure in the piston-cylinder system. To determine the piston speed, the distance traveled between top dead center (TDC) and bottom dead center (BDC) is calculated. In an internal combustion engine, the piston undergoes four strokes, requiring it to travel four times the stroke length. This corresponds to a total crank angle of 720 degrees. The 720-degree crank angle represents the number of angular positions at which the piston is evaluated and allows for a more accurate assessment of engine performance.

Additionally, it is used to calculate fluid film thickness for effective lubrication. Equation (8) is employed to calculate the piston velocity, enabling a comprehensive analysis of piston movement, lubrication requirements, and overall engine performance.

$$U_{avg} = R\text{w}^2\left[sin\theta + \frac{R}{2L}sin2\theta\left(1 - \left(\frac{R}{L}\right)^2 sin^2\theta\right)\right] \quad (8)$$

Film Thickness

In hydrodynamic lubrication, the film thickness is determined using Equation (9), where H represents the total film thickness consisting of the minimum film thickness h_{min} , and the ring profile h_s. The ring profile h_s, is calculated based on the ring geometry using the equation (10), where C is the crown height, o is the crown offset from the ring center, and b is the ring width [5].

$$H = h_{min} + h_s \quad (9)$$

$$h_s = \frac{C}{\left(\frac{b}{2}+o\right)^2}(x-o)^2 \quad (10)$$

Combustion Pressure and Load

Combustion pressure is a crucial factor in this study as it directly influences the forces exerted by the piston ring on the cylinder liner. It originates from the ignition of the fuel-air mixture, resulting in the production of high-pressure gases that drive the piston downward during the power stroke. The combustion pressure data used in this study is obtained through experimental analysis [5].

The combustion pressure is converted into a load that acts on the compression ring, exerting a pushing force. This relationship is represented by Equation (11), where the combustion pressure serves as the driving force and the ring area represents the contact area between the compression ring and the cylinder liner.

$$Load = Rw\left[\frac{2T}{(Rw)(Bore)}\,Pressure\right] \quad (11)$$

By considering combustion pressure and ring tension, the load exerted by the piston ring on the cylinder liner can be calculated.

Friction Model

This load introduces friction between the ring and liner, classified as boundary and viscous friction. Equation (13) represents total friction F_f as the sum of boundary F_b and viscous F_v friction.

$$F_f = F_b + F_v \quad (12)$$

To calculate total friction force F_f, the Greenwood and Tripp rough surface contact model [12] is used. This model assumes Gaussian distribution of asperity heights and constant radius of curvature, determining the contact area and A_a load P_a.

$$A_a = \Pi^2(\zeta\beta\sigma)^2 AF_2(\lambda) \quad (13)$$

$$P_a = \frac{8\sqrt{2}}{15}\Pi(\zeta\beta\sigma)^2\sqrt{\frac{\sigma}{\beta}}E^*AF_{5/2}(\lambda) \quad (14)$$

The combined asperity of the two surfaces, represented by σ, along with the separation parameter λ and statistical functions F_2 and$F_{5/2}$, can be calculated using the RMS asperity heights $\sigma_1$and σ_1.

$$\lambda = \frac{h}{\sigma} \quad (15)$$

$$\sigma = \sqrt{\sigma_1^2 + \sigma_2^2} \quad (16)$$

where

$$F_{5/2} = -0.1922\lambda^3 + 0.721\lambda^2 - 1.0649\lambda + 0.6163 \quad (17)$$

$$F_2 = -0.116\lambda^3 + 0.4862\lambda^2 - 0.7949\lambda + 0.4999 \quad (18)$$

$$\frac{1}{E^*} = \frac{1}{2}\left[\frac{1-v_1^2}{E_1} + \frac{1-v_2^2}{E_2}\right] \quad (19)$$

Boundary friction force, F_b refers to the resistance encountered due to the interaction between the rough surfaces of the piston ring and the cylinder liner. It can be calculated using Equation (20).

$$F_b = \tau_0 A_a + mP_a \quad (20)$$

where the τ_0 represent the Eyring stress of the lubricant oil, which is about 2 MPa, m represent the pressure coefficient of boundary shear strength which about 0.17.

Meanwhile, viscous friction, F_v is related to the shearing resistance of the lubricating film present between the piston ring and the cylinder liner. It can be calculated using Equation (21).

$$F_v = \tau(A - A_a) \quad (21)$$

For both friction, $\tau = \eta V/h$. In addition, if $\tau > \tau_0$, the shear stress τ is determined by:

$$\tau = \tau_0 + \gamma p^* \quad (22)$$

where p^* refers to the pressure on the lubricant oil film.

Results and Discussion

Simulation Input Parameters

The study utilizes existing literature data to validate piston ring, lubrication, and engine operating conditions. Lubrication pressure distribution at the piston ring-cylinder liner conjunction is determined using the 1-D Reynolds equation with an estimated initial lubricant viscosity. A C-programming-based friction model is developed to investigate friction properties. Additionally, the study examines the impact of viscosity degradation and a worn top compression ring on friction by incorporating these factors into the analysis.

The simulation input values in Table 1 are based on Jeng's study [3], where combustion pressure and piston velocity data were extracted. The combustion pressure values were obtained using Web Plot Digitizer. The resulting piston ring load and calculated piston velocity are shown in Figures 1 and 2.

Table 1: Simulation input parameters

Parameters	Value
Bore, B (mm)	88.9
Half Stroke, R (mm)	40.0
Rod Length, L (mm)	141.9
Composite Roughness, σ (μm)	0.37
Initial Lubricant Viscosity, η (Pa.s)	0.00689
Speed, s (rpm)	2000
Width, b (mm)	1.475
Crown Height, C (μm)	14.9
Offset, o (mm)	0.0
Tension, T (N)	22.38

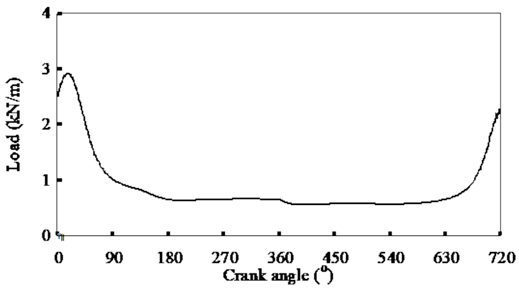

Figure 1: Load imposed on top compression ring

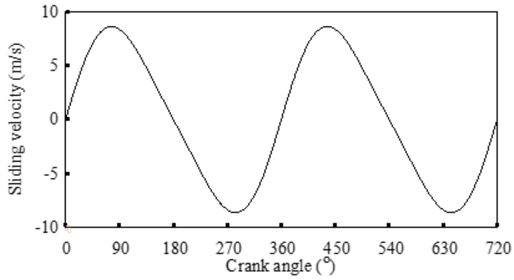

Figure 2: Piston sliding velocity

Number of Nodes

To increase the accuracy of film thickness and pressure distribution along the width, the number of nodes chosen is crucial. To determine the most suitable number of nodes for the ring width at different crank angles, a comparative analysis is conducted using two high-speed crank angles, namely 76° and 436°, as given in Table 2 and 3. The analysis determined that a number of nodes resulting in a percentage difference below 3% is considered acceptable, ensuring accurate results.

Table 2: Node sensitivity analysis at crank angle 76°

Node number	Peak press. (MPa)	% Change	Min. film thick. (μm)	% Change
40	3.773	-	1.696	-
60	3.845	1.9	1.611	5.0
80	3.912	1.8	1.568	2.7
100	3.942	0.8	1.542	1.7

Table 3: Node sensitivity analysis at crank angle 436°

Node number	Peak press. (MPa)	% Change	Min. film thick. (μm)	% Change
40	1.568	-	2.835	-
60	1.602	2.2	2.716	4.2
80	1.615	0.8	2.669	1.7
100	1.623	0.5	2.623	1.7

Comparing Tables 2 and 3, it can be concluded that employing 80 nodes provides reliable predictions of film thickness and pressure distribution. This specific number optimizes accuracy, allowing for better understanding of lubrication performance and friction characteristics in the piston ring-cylinder liner conjunction.

Frictional Characteristics

The input values for the friction model are provided in Table 4. The graph represents the combined effect of boundary friction and viscous friction.

Table 4: Input parameters for friction model

Parameter	Value
$\zeta\beta\sigma$	0.03
$\frac{\sigma}{\beta}$	0.001
τ_0	2 MPa
m	0.08
γ	0.08

Peaks observed in Figure 3 (a) indicate the dominance of boundary friction at those locations. Boundary friction occurs when two surfaces are in direct contact. Figure 3 (a) shows that frictional forces between the piston rings and cylinder liner are not constant throughout the engine cycle. They vary based on operating conditions such as load and piston velocity.

At higher speeds (mid span stroke at every 90° crank angle), frictional forces may increase due to greater relative motion and higher oil film shear stresses, resulting in higher viscous friction (Figure 3 (b)). Conversely, at low speeds, frictional forces may be higher due to reduced lubricant film thickness, leading to increased boundary friction (Figure 3 (c)).

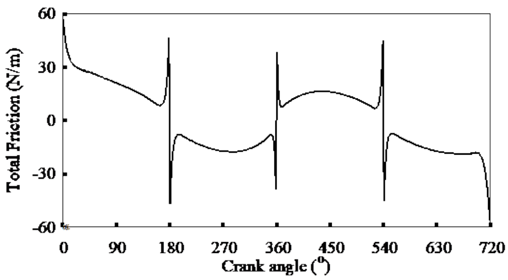

(a) Total Friction

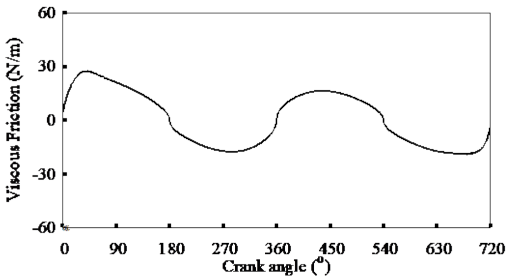

(b) Viscous Friction

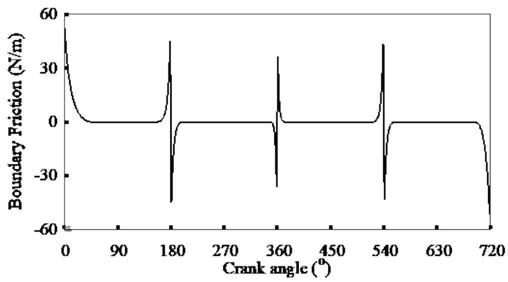

(c) Boundary Friction

Figure 3: Friction at top compression ring

Lubricant Degradation

Lubricant degradation is studied, particularly the influence of changing viscosity. The simulation considers a degradation scenario where the lubricant experiences a 20% and 40% increase in viscosity compared to its initial value, as listed in Table 5. Increased viscosity is commonly associated with combustion by-product contamination and lubricant oxidation.

Table 5: Input parameters for lubricant degradation analysis

Case	Initial Lubricant Viscosity (Pa.s)
#1	0.00689
#2	0.00827
#3	0.00965

Figure 4 shows that higher lubricant viscosity increases film thickness, providing better surface protection under high loads. Lubricant degradation significantly impacts film thickness and friction between the piston ring and cylinder liner.

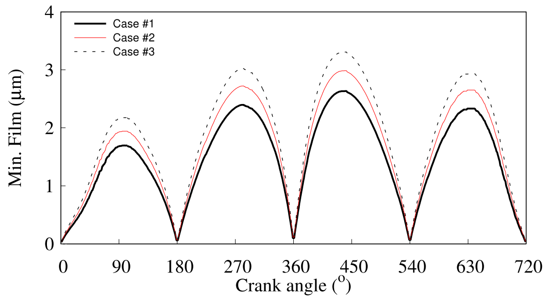

Figure 4: Lubricant minimum film thickness for top compression ring at different levels viscosity degradation

Figure 5 demonstrates friction at different viscosities throughout the engine cycle, while Figure 6 highlights reduced friction at TDC and BDC due to increased viscosity and thicker film separation.

In Figure 7, viscous friction reveals that friction increases during the mid-span stroke. This is due to the higher viscosity of the lubricant, leading to higher shear stress within the lubricating film. Increased viscosity creates more resistance to flow, resulting in elevated shear stress and overall higher viscous friction. Compared to the initial lubricant viscosity without any increase, the viscous friction is lower.

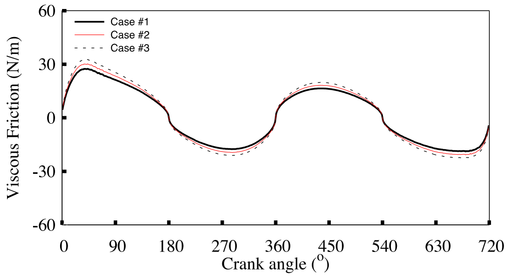

Figure 7: Boundary friction for top compression ring at different levels viscosity degradation

Worn Top-Compression Ring

To consider the effect of worn piston ring, the ring geometry in Equation (9) is modified into Equation (22) below:

$$h_s = \frac{C}{(n-1)\left(\frac{b}{2}+o\right)^n}(x-o)^n \tag{22}$$

where *n* is the polynomial coefficient introduced to simulate the extend of piston ring wear at the tip. The simulated value for *n* is tabulated in Table 6. The ring profile is plotted in Figure 8, where the tip is shown to experience more wear with larger *n* values, giving rise to a flatter tip.

Table 6: Input parameters for worn top compression ring analysis

Case	Polynomial coefficient (n)
#1	2
#2	2.5
#3	3.0

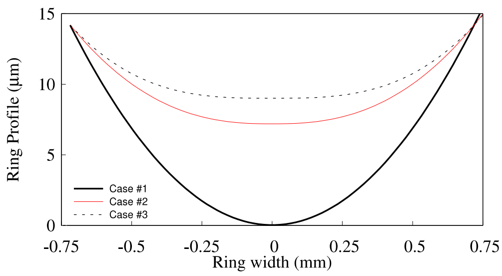

Figure 8: Top compression ring profile at different worn conditions

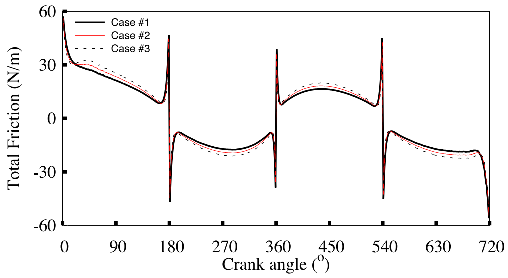

Figure 5: Total friction for top compression ring at different levels viscosity degradation

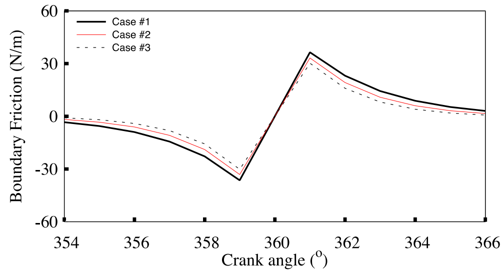

Figure 6: Boundary friction for top compression ring at different levels viscosity degradation (top dead centre during intake stroke)

Figure 9 shows how a worn top compression ring increases lubricant film thickness during the mid-span stroke, especially in regions with more severe wear. This is due to the presence of a flatter ring tip that enhances load carrying capacity.

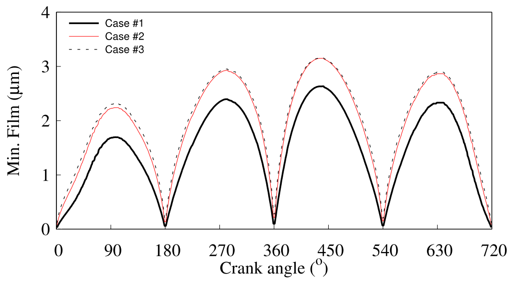

Figure 9: Lubricant minimum film thickness for top compression ring at different levels of ring wear

Figure 10 illustrates the contact pressure distribution along the ring, indicating a lower peak pressure but a larger load-bearing area for the worn ring, capable of sustaining higher loads.

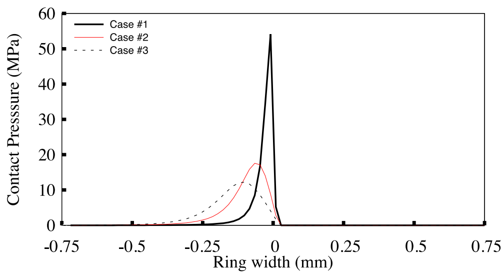

Figure 10: Top compression ring contact pressure at different worn conditions at 0° crank angle

Figure 11 displays friction between the piston ring and cylinder liner under different wear conditions. Higher friction is observed in regions corresponding to the mid-span stroke for rings with more severe wear, primarily due to increased viscous friction.

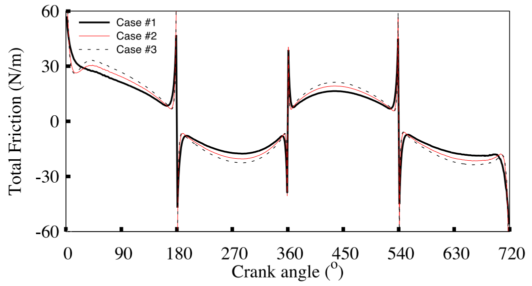

Figure 11: Total friction for top compression ring at different levels of ring wear

Figure 12 further demonstrates that worn rings exhibit larger viscous friction due to thicker film formation and a larger load-bearing area.

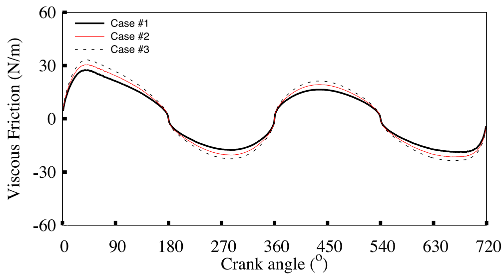

Figure 12: Boundary friction for top compression ring at different levels of ring wear

Conversely, Figure 13 shows a reduction in boundary friction, resulting from the thicker film that separates the ring and liner, reducing surface asperity interactions. In summary, the worn top compression ring significantly influences friction by affecting film formation and lubricant distribution within the contact area. It directly impacts hydrodynamic pressure and contributes to the formation of the lubricating film.

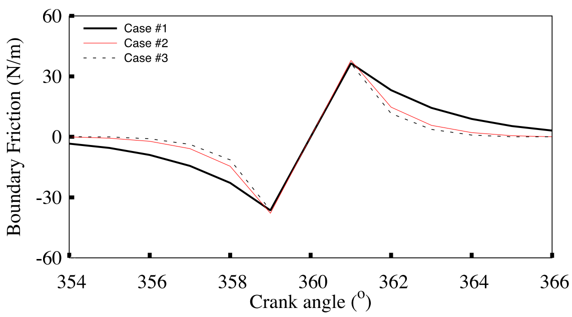

Figure 13: Boundary friction for top compression ring at different levels of ring wear (top dead centre during intake stroke)

Comparative Study

The conversion of friction between the piston ring and cylinder liner into frictional power losses. Friction is measured at each crank angle and then multiplied by the corresponding velocity to calculate friction power. Table 7 compares friction power considering lubricant degradation via viscosity change. It demonstrates that as the lubricant degrades, leading to increased viscosity, friction power losses for the top compression ring also increase. Linear regression analysis estimates that a 1% increase in viscosity corresponds to a 0.45% increase in friction power.

On the other hand, Table 8 compares the change in friction power for different levels of ring wear. Wear volume is calculated by measuring the volume difference between various ring profiles depicted in Figure 13.

It is crucial to acknowledge that ring wear results in an increase in friction power loss. Linear regression analysis indicates that a 1% increase in ring wear volume corresponds to a 0.35% increase in friction power.

Table 7: Friction power comparison for lubricant degradation analysis

Case	Initial Lubricant Viscosity (Pa.s)	Changes (%)	Total Friction Power (kW/m)	Changes (%)
#1	0.00689		65.3	
#2	0.00827	20	71.3	9.2
#3	0.00965	40	77.1	18.1

Table 8: Friction power comparison for different levels of ring wear

Case	Polynomial coefficient (n)	Changes (%)	Total Friction Power (W/m)	Changes (%)
#1	2		65.3	
#2	2.5	45	73.7	12.9
#3	3.0	60	80.7	23.6

Conclusion

In this study, a mathematical model for the lubrication of the top compression ring is derived by solving the 1-D Reynold's equation. By integrating friction models, relative velocity, lubrication degradation, combustion load, and input parameters of the worn top compression ring, frictional losses are determined. Factors such as lubricant viscosity, combustion load, relative velocity, and ring profile influence the formation of the lubricating film thickness and subsequently affect the friction generated.

A full engine cycle analysis covering 720° of crank angle evaluates the impact of these factors. The study reveals that lubrication degradation increases viscous friction and decreases boundary friction, while a worn top compression ring increases viscous friction but reduces boundary friction. Friction values are converted into frictional power losses by multiplying with the relative velocity. Lubricant degradation and worn rings both contribute to higher friction power losses, with estimated percentage increases corresponding to viscosity and ring wear volume. Proper maintenance practices, regular lubricant changes, and timely replacement of worn rings are essential to minimize frictional losses and ensure optimal engine performance.

The mathematical model in this study for piston ring and cylinder liner conjunction can be further improved with following recommendations:

- Consideration of squeeze film effect and combustion blow by.
- Consideration of starvation or cavitation between the lubrication oil film.
- Consideration of lubricant rheology to change with contact pressure, such as the non-Newtonian flow behaviour.

Acknowledgements

This work was supported by Higher Institution Centre of Excellence (HiCOE) program of Ministry of Higher Education (MOHE) Malaysia under HiCOE Research Grant R.J130000.7824.4J741.

Conflict of Interest

The author declares that there is no conflict of interest regarding the publication of this paper.

References

[1] Menacer, B., & Bouchetara, M. (2020). The compression ring profile influence on hydrodynamic performance of the lubricant in diesel engine. *Advances in Mechanical Engineering, 12*(6), 168781402093084. https://doi.org/10.1177/168781402093084

[2] Turnbull, R., Dolatabadi, N., Rahmani, R., & Rahnejat, H. (2020). An assessment of gas power leakage and frictional losses from the top compression ring of internal combustion engines. *Tribology International, 142*, 105991.

[3] Rahmani, R., Theodossiades, S., Rahnejat, H., & Fitzsimons, B. (2012). Transient elastohydrodynamic lubrication of rough new or worn piston compression ring conjunction with an out-of-round cylinder bore. *Proceedings of the Institution of Mechanical Engineers, Part J: Journal of Engineering Tribology, 226*(4), 284–305.

[4] Styles, G., Rahmani, R., Rahnejat, H., & Fitzsimons, B. (2014). In-cycle and life-time friction transience in piston ring–liner conjunction under mixed regime of lubrication. *International Journal of Engine Research, 15*(7), 862–876.

[5] Jeng, Y.-R. (1992). Theoretical analysis of piston-ring lubrication Part I—Fully flooded lubrication. *Tribology Transactions, 35*(4), 696–706.

[6] Morris, N. A., Rahmani, R., Rahnejat, H., King, P. J., & Howell-Smith, S. J. (2015). A numerical model to study the role of surface textures at top dead center reversal in the piston ring to cylinder liner contact. *Journal of Tribology, 138*(2).

[7] Söderfjäll, M., Herbst, H. M., Larsson, R., & Almqvist, A. (2017). Influence on friction from piston ring design, cylinder liner roughness and lubricant properties. *Tribology International, 116*, 272–284.

[8] Morris, N., Rahmani, R., Rahnejat, H., King, P., & Fitzsimons, B. (2012). The influence of piston ring geometry and topography on friction. *Proceedings of the Institution of Mechanical Engineers, Part J: Journal of Engineering Tribology, 227*(2), 141–153.

[9] Sonthalia, A., & Kumar, C. (2013). The effect of compression ring profile on the friction force in an internal combustion engine. *Tribology in Industry, 35*(1), 74–83.

[10] Jadhav, N. (2013). Friction losses between piston ring–liner assembly of internal combustion engine: A review. *International Journal of Scientific and Research Publications, 3*(6).

[11] Balakrishnan, S., & Rahnejat, H. (2005). Isothermal transient analysis of piston skirt-to-cylinder wall contacts under combined axial, lateral and tilting motion. *Journal of Physics D: Applied Physics, 38*(5), 787–799.

[12] Teodorescu, M., Taraza, D., & Henein, N. A. (2003). Simplified elasto-hydrodynamic friction model of the cam–tappet contact. *JSTOR*. https://www.jstor.org/stable/44741353